ON SPATIO-TEMPORAL PATTERNS IN TWO-LAYER RING TOPOLOGY NEURAL FIELDS

Fayssa Salomon
Evan C Haskell
Division of Math, Science, and Technology
Farquhar College of Arts and Sciences
Nova Southeastern University
Fort Lauderdale, FL 33314 USA
haskell@nova.edu

ABSTRACT

Spatially coherent structures and propagating waves of neural activity are commonly found throughout the central nervous system. These activity profiles are represented in both natural and pathological phenomena. We explore a two-layer neural field model dually constrained by local interactions and a cortical topography described by a ring topology neural network. We examine the conditions for the generation of wave solutions. The constraints on neuronal network computation implied by the dual local constraints may place further constraints on global cortical network architecture to achieve physiologically consistent wave behavior.

INTRODUCTION

Spatially coherent activity states are ubiquitous throughout the central nervous system and in observations from voltage-sensitive dye imaging (VSDI) and multi-electrode arrays (Wu et al., 2008). These patterns including localized activity states, spatially homogeneous oscillations, and wave behavior, may play important roles in neo-cortical processing and nervous system development. These behaviors can arise as an emergent behavior from interacting neural populations (Amari, 1977; Wu et al., 2008). Recurrent network connections have long been proposed as a mechanism for the formation of such patterns observed in many phenomena including feature selectivity in the visual system (Somers et al., 1995; Hansel and Sompolinsky, 1998), working memory (Amit and Brunel, 1997), head direction system (Zhang, 1996), motion perception (Giese, 1998), and in describing EEG rhythms (Nunez, 1995), local field potential spectra (Pinotsis et al., 2012), and wave behavior (Coombes, 2005). Understanding the mechanisms that contribute to the generation of such patterns is important for understanding a host of both natural and pathologic neurobiological behaviors. Propagating waves are observed as sensory evoked waves in cortex, epileptiform waves underlying epileptic seizures, and spontaneous waves of cortical activity, the latter may be of particular import for cortical processing (Wu et al., 2008).

In this report we follow a framework for studying spatially coherent structures and waves of activity in neural fields introduced by Amari (Amari, 1977). Amari demonstrated how the predominantly local interactions in neural populations give rise to localized activity states, oscillations, and stationary traveling waves of activity in a neural field model defined over the real line. Such neural field models are tissue level descriptions of mean membrane potential. In addition to local interactions, topographic maps of sensory features are ubiquitous in cortical sensory systems and some motor systems and may play fundamental roles in sensory processing (Woolsey et al., 1942; Hubel and Wiesel, 1977; Kass, 1997; Silver and Kastner, 2009; Wilimzig et al., 2012). These maps provide a functional network architecture that we explore within the neural field framework presented by Amari. Advances in VSDI have allowed for the in vivo measuring of population responses in superficial cortical layers at high spatial and temporal resolution (Grinvald and Hildesheim, 2004). Taking a cue from the columnar topographic organization of the topographic map for orientation tuning in primate cortex (Blasdel and Salama, 1986) we explore ring topology neural fields.

The interaction of local processing by neural networks and stimulus topography places a strong constraint on cortical processing. Distributions of preferred features may maximize sensitivity throughout the stimulus space (Purushothaman and Bradley, 2004). It has been proposed in primary visual cortical area V1 that the structure of natural stimuli may well serve to shape the network architecture in area V1 (Simoncelli and Olshausen, 2001; Singh et al., 2008). For associative learning tasks, the interaction of local processing and topography may result in a biased distribution of preferred stimulus (Fitzgerald et al., 2013). Indeed, the interaction of local processing and compact topologies implied solely by regular topography of cortical regions for feature selectivity has demonstrated new results for single layer neural fields (Haskell and Bressloff, 2003; Haskell and Paksoy, 2011). We provide a taxonomy of standing wave solutions in two layer neural fields showing that regions of tri-stability observed in single layer fields are also observable in two layer neural fields. We point out that the topology of feature space does not play a factor in homogeneous oscillations but owing to the periodic nature of the ring topology prohibits the formation of traveling front solutions which are observable in single layer neural fields defined over the real line.

NEURAL FIELD MODEL

Subthreshold level neuronal activity is reflected in recordings from VSDI that represents local mean membrane potential. From the VSDI measurement a prediction of spiking activity by neurons can be made (Chen et al., 2012). The local network processing of this spiking activity results in many emergent behaviors including localized activity states, oscillations, and propagating waves of neural activity (Amari, 1977; Coombes, 2005).

For our model, we consider a continuum of neurons distributed on a ring domain indexed by a stimulus variable $\theta \in [-\pi, \pi)$. Here θ may represent for example the orientation selectivity of a neuron in cortical area V1 which maps directly by the topography of V1 to a continuous position variable. The evolution equation for the mean membrane potential, $u_i(\theta, t)$, for neurons in a m layer network indexed by i receiving a homogenous external input h_i and an inhomogeneous external input $s_i(\theta, t)$ is of the form:

$$\tau_i \frac{\partial u_i(\theta, t)}{\partial t} = -u_i(\theta, t) + h_i + s_i(\theta, t)$$
$$+ \sum_{j=1}^{m} \int_{-\pi}^{\pi} w_{ij}(\theta|\theta') f[u_j(\theta', t)] \frac{d\theta'}{2\pi} \quad (1)$$

where $w_{ij}(\theta|\theta')$ is a connectivity function representing the mean synaptic efficacy from a neuron at a position θ' in layer j to a neuron at position θ in layer i, $f[u_i]$ is a transduction function from the mean membrane potential, u_i, to the mean rate of spiking activity or activity level and $\tau_i > 0$ is the time constant for the dynamics of the type of neuron represented in layer i, $f[u]$ should be a non-decreasing saturating function. The simplest choice that exhibits non-trivial dynamics is a Heaviside function where the neuron is fully active when the mean membrane potential is above a firing threshold and inactive otherwise (Amari, 1977; Coombes, 2005; Haskell and Bressloff, 2003; Haskell and Paksoy, 2011). As such, we choose such a function for the analysis presented below:

$$f[u] = \begin{cases} 1 & \text{if } u > 0 \\ 0 & \text{otherwise} \end{cases} \quad (2)$$

Experimental evidence suggests that local circuits operate with neurons connecting to most of their neighbors in a manner that is approximately isotropic and homogeneous (Douglas et al., 1995) as such, we consider a connectivity function $w_{ij}(\theta|\theta')$ that depends only on the relative distance in the case of a position variable or feature dissonance in the case of a feature variable between neurons. In the ring topology this is measured as angular separation, $\theta - \theta'$ (Ben-Yishai et al., 1995; Somers et al., 1995; Haskell and Bressloff, 2003). As well, experimental evidence in orientation preference maps suggests that intracortical excitatory and inhibitory synaptic currents are distributed with differences in preferred orientation (Roerig and Chen, 2002). This homogeneity of the neural field implies

a rotational symmetry for the connectivity function that is invariant to the $O(2)$ symmetry group of coordinate rotations and reflections in the ring. Thus $w_{ij}(\theta|\theta')$ with $w_{ij}(\theta)$ a 2π-periodic even function of θ, $w_{ij}(\theta) = w_{ij}(\theta + 2\pi) = w_{ij}(-\theta)$. Any such connectivity function can be written as a cosine series expansion:

$$w_{ij}(\theta) = W_0^{ij} + \sum_{k>0} W_k^{ij} \cos(k\theta)$$

Considering only the first two terms of the expansion,

$$w_{ij}(\theta) = W_0^{ij} + W_1^{ij} \cos(\theta),$$

is sufficient for non-trivial results (Ben-Yishai et al., 1997; Haskell and Bressloff, 2003; Haskell and Paksoy, 2011). Single layer neural fields (m=1) of lateral inhibition type and ring topology with only first two components of the weighting kernel have previously been demonstrated to exhibit stable localized activity states where only a local region of the neural field is active (Haskell and Bressloff, 2003; Haskell and Paksoy, 2011). Lateral inhibition type neural fields correspond to a local connectivity where neurons in close proximity are mutually excitatory while those more distal are mutually inhibitory requiring $W_1^{11} > W_0^{11}$ and $W_0^{11} + W_1^{11} > 0$. When $W_0^{ii} > W_1^{ii} > 0$ for a layer i, the layer is self excitatory.

The discrete layers can be used to represent the heterogeneity of neurons collocated in a cortical tissue. Differences in effective membrane properties and synaptic filtering and latency would be encapsulated respectively in the membrane time constant, τ_i, and time-dependent synaptic efficacy function, $w_{ij}(\theta_i, \theta_j, t)$. Studies of the general properties of cortical networks commonly pool neurons into two layers representing excitatory cells and inhibitory cells respectively (Wilson and Cowan, 1973; Amari, 1977; Haskell and Bressloff, 2003; Haskell and Paksoy, 2011; Ben-Yishai et al., 1997; Pinto and Ermentrout, 2001; Blomquist et al., 2005). To study the formation of spatio-temporal patterns in a topographically constrained network with local interactions, we consider the system (1) with $m = 2$ as a two layer neural field (Amari, 1977; Ben-Yishai et al., 1997; Salomon and Haskell, 2012).

For the two layer neural field we utilize the Amari type connectivity where the excitatory neurons (layer 1) receives input from both layers 1 and 2; while, inhibitory neurons (layer 2) receive only excitatory input from neurons in layer 1 that share the same position variable θ ($W_1^{21} = 0$). Thus the two layer version of system (1) may be written as:

$$\tau_1 \frac{\partial u_1}{\partial t} = -u_1(\theta, t) + \int_{-\pi}^{\pi} w_{11}(\theta - \theta') f[u_1(\theta', t)] \frac{d\theta'}{2\pi}$$
$$- \int_{-\pi}^{\pi} w_{12}(\theta - \theta') f[u_2(\theta', t)] \frac{d\theta'}{2\pi} + h_1$$
$$\tau_2 \frac{\partial u_2}{\partial t} = -u_2(\theta, t) + W_0^{21} f[u_2(\theta, t)] + h_2 \quad (3)$$

In order to prevent layer 2 from being persistently fully active (i.e. $u_2(\theta, t) > 0, \forall \theta\ t$) we require $h_2 < 0$; however, for layer 2 to be able to provide feedback to layer 1 we must have $W_0^{21} > -h_2$.

A segregation of the collocated neurons into a layer of excitatory (layer 1) and inhibitory (layer 2) neurons corresponds to $W_0^{11} > W_1^{11}$ and $W_0^{12} > W_1^{12}$. Note that for the description of the connectivity function the excitatory and inhibitory interactions are maximal for neurons with similar feature preference consistent with experimental findings (Roerig and Chen, 2002). In the visual cortex of ferret it has been demonstrated that the overwhelming majority of cortical inputs are local with excitatory inputs being very narrowly tuned to the orientation preference of the cells and inhibitory inputs showing a broader tuning with excitatory post-synaptic currents being dominant from cells with similar orientation preference and inhibitory post-synaptic currents dominant for cells with dissimilar orientation preference (Roerig and Chen, 2002). This is modeled in the two layer neural field (3) by setting $W_0^{11} + W_1^{11} > W_0^{12} + W_1^{12}$ and $W_0^{11} - W_1^{11} < W_0^{12} - W_1^{12}$. Note that in the ferret study the excitatory connections are localized to stimulus feature but not physical location. That is, the connections span across the cortical hypercolumn to the next patch of neurons with similar orientation preference. As such, from a computational perspective, the periodic boundary conditions provide an extension to a periodic media. That is, the traveling wave solutions we find are traveling periodic pulses in sense that $u_i(\theta, t - t_0) = u_i(\theta + vt_0, t)$ where v is an unknown wave velocity and $\theta + vt_0$ is understood to be appropriately shifted by a multiple of 2π (Shigesada and Kawasaki, 1997).

STANDING WAVES

Standing waves manifest as equilibrium solutions, $u_i(\theta, t) = U_i(\theta)$, with continuous regions where the field is active within a given region and inactive outside that region. The active region of the field is characterized by the set function:

$$R[U_i] = \{\theta | U_i(\theta) > 0\}.$$

Two layer Wilson-Cowan equations have been shown to present paired pulse solutions over the real line (Pinto and Ermentrout, 2001; Blomquist et al., 2005) and in ring topologies (Ben-Yishai et al., 1997). For single layer neural field models with compact network topologies and connectivity functions modeled by first order harmonics, a full taxonomy of the localized activity states demonstrates parameter regimes of tri-stability and ability to form localized activity states with homogenous excitatory input (Haskell and Bressloff, 2003; Haskell and Paksoy, 2011). In this section we extend that discussion to the two layer ring topology setting and show regimes of tri-stability and paired pulse solution with homogeneous excitatory input.

Following the Amari analysis for the formation of localized activity states in a single layer, we construct a pair of standing pulse solutions (Amari, 1977; Pinto and Ermentrout, 2001; Blomquist et al., 2005). Without loss of generality we consider the standing pulse in layer 1 to be centered at $\theta = 0$ with an unknown width $2a < 2\pi$, that is, $R[U_1] = (-a, a)$. For $W_0^{21} > -h_2$ we find $R[U_2] = (-a, a)$ otherwise $R[U_2] = \emptyset$. The time independent solution for layer 2 is:

$$U_2(\theta) = \begin{cases} W_0^{21} + h_2 & -a < \theta < a \\ h_2 & \text{otherwise} \end{cases}$$

and layer 1:

$$U_1(\theta) = \frac{1}{\pi}\Big((W_0^{11} - W_0^{12})a$$

$$+ (W_1^{11} - W_1^{12}) \sin(a) \cos(\theta) \Big) + h_1. \qquad (4)$$

The unknown value a is then found by solving the relation $U_1(\pm a) = 0$. As $U_i(\theta)$ is an even function, it is sufficient to consider only $\theta = a$ and seek solutions of

$$W(a) + h_1 = 0$$

where,

$$W(a) = \frac{1}{\pi}\Big((W_0^{11} - W_0^{12})a + \frac{W_1^{11} - W_1^{12}}{2}\sin(2a) \Big). \quad (5)$$

We extend to two layer neural field setting our previous found implications of (5) for single layer neural fields in compact topologies (Haskell and Bressloff, 2003; Haskell and Paksoy, 2011).

Theorem 1: In the absence of inhomogeneous input:
a) There exists a quiescent state if and only if $h_1 < 0$.
b) There exists a fully active state if and only if
   $W_0^{11} > W_0^{12} - h_1$.
c) There exists a standing wave if and only if
   $W(a) + h = 0$ for some $a \in (0, \pi)$ and $W_1^{11} > W_1^{12}$.
Proof:
a) The quiescent state corresponds to no activity in layer 1 or 2 so that $R[U_1] = \emptyset, R[U_2] = \emptyset$ implying $U_1(\theta) = h_1$ and $U_2(\theta) = h_2$. This requires $h_1 < 0$. From the model assumptions $h_2 < 0$. If $h_1 < 0$ then $U_1(\theta) = h_1$ yields a quiescent state to the system.
b) A fully active state corresponds to $R[U_1] = [-\pi, \pi)$. This implies that $U_1(\theta) = W_0^{11} - W_0^{12} + h_1$ and $U_2(\theta) = W_0^{21} + h_2$. This requires the mean drive a neuron receives from recurrent connections in layer 1 to be greater than the net mean input the neuron receives from layer 2 and the homogeneous drive, that is, $W_0^{11} > W_0^{12} - h_1$. Note that $W_0^{21} + h_2 > 0$ by model assumption. If $W_0^{11} > W_0^{12} - h_1$ then $U_1(\theta) = W_0^{11} - W_0^{12} + h_1$ is a fully active state.
c) For $R[U_i] = (-a, a), i = 1, 2, U_1(\theta) > 0$ for $-a < \theta < a, U_1(\theta) < 0$ for $a < |\theta| < \pi$, and $U_1(\theta) = 0$ for $\theta = \pm a$. Such a solution with $U_1(\theta) = 0$ for $\theta = \pm a$ occurs if and only if $W(a) + h = 0$. Noting that (4) is a monotonically decreasing (increasing) function for $W_1^{11} > W_1^{12}$ $(W_1^{11} < W_1^{12})$ then $U_1(\theta) < 0$ for $a < |\theta| < \pi$ requires $W_1^{11} > W_1^{12}$.

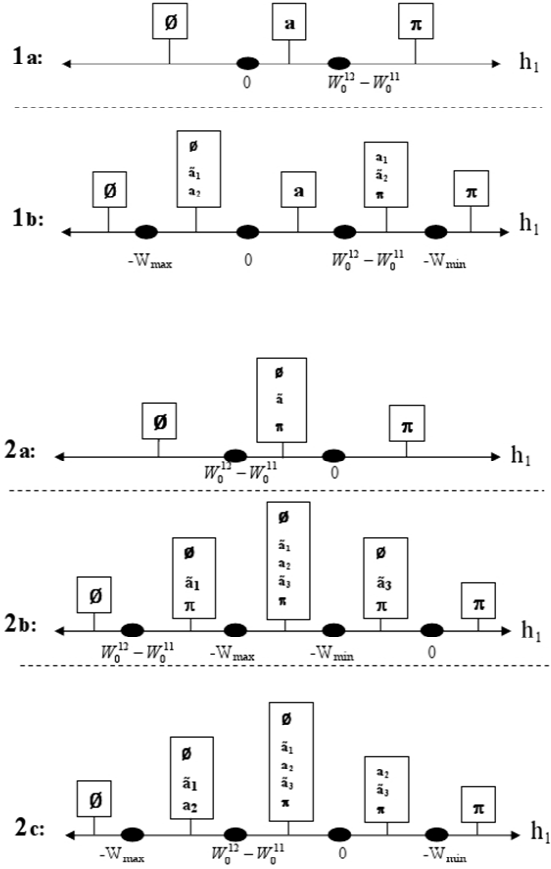A taxonomy for the standing wave solutions summarized in figure 1 derives from the existence requirement

Fig. 1. Equilibrium solutions for various values of h_1. The existence of quiescent ($\emptyset$), fully active (π), and localized activity states ($a_i, a_1 < a_2 < a_3$) are indicated with the corresponding range of h_1 indicated. Unstable localized activity states are indicated with a tilde.

that the modulation of the mean input a layer 1 neuron receives from recurrent connections within layer 1 exceed that received from layer 2 ($W_1^{11} > W_1^{12}$). These solutions can be separated into two distinct cases where the mean input from recurrent connections within layer 1 exceeds or is exceeded by that received from layer 2. Respectively these two cases are represented by case 1 where $W_0^{11} > W_0^{12}$ and case 2 where $W_0^{11} < W_0^{12}$.

Case 1a: $W_0^{11} + W_1^{11} < W_0^{12} + W_1^{12}$: In this case $W(a)$ has no stationary points and is a monotonically decreasing function. There is a standing wave when $0 < h_1 < W_0^{21} - W_0^{11}$.

Case 1b: $W_0^{11} + W_1^{11} > W_0^{12} + W_1^{12}$: $W(a)$ has two stationary points with $W_{max} > 0 > W_{min}$ where W_{max} and W_{min} indicate the maximum and minimum values of $W(a)$ respectively. There are two regions of bistability with the standing wave and either the quiescent or fully active state both stable.

Case 2a: $0 < W_1^{11} - W_1^{12} < W_0^{11} - W_0^{12}$: $W(a)$ has no stationary points and is a monotonically increasing function. There is no stable standing wave; however there is a region with an unstable standing wave separating a stable quiescent and all active state.

Case 2b: $W_0^{11} - W_0^{12} < W_1^{11} - W_1^{12} < \gamma(W_0^{11} - W_0^{12})$: $W(a)$ has two stationary points with $W_{min} > 0$. We find not just regions of mono- and bi-stability with the quiescent or all active state but also a region of tri-

stability when $-W_{max} < h_1 < W_{min}$ where stable quiescent and all active states are found along with a stable standing wave. The value $\gamma \approx 4.6$ separates the region where $W_{min} > 0$ and $W_{min} < 0$ is found numerically (Haskell and Paksoy, 2011).

Case 2c: $\gamma(W_0^{11} - W_0^{12}) < W_1^{11} - W_1^{12}$: As in 2b $W(a)$ has two stationary points with $W_{max} > 0 > W_{min}$. We again find regions of mono-, bi-, and tri-stability. We note that there is a region of bi-stability between the localized activity state and the fully active state for some positive h_1 values.

In the development of the two-layer field model, we required both $h_2 < 0$ and $W_0^{21} > -h_2 > 0$. Relaxing either of these requirements reduces the question of standing pulses in layer 1 to the case we previously studied for single layer neural fields with compact topology (Haskell and Bressloff, 2003; Haskell and Paksoy, 2011). In the case where $h_2 < 0$ and $W_0^{21} < -h_2$ we find $R[U_2] = \emptyset$ and $W(a) = \frac{1}{\pi}\left(W_0^{11}a + \frac{W_1^{11}}{2}\sin(2a)\right)$. In the case where $h_2 > 0$ and $W_0^{21} > 0$ we find $R[U_2] = S^1$ and $W(a) = \frac{1}{\pi}\left(W_0^{11}a + \frac{W_1^{11}}{2}\sin(2a) - W_0^{12}\right)$. In this latter special case finding solutions to $W(a) + h_1 = 0$ effectively shifts the values of h_1 that separate different equilibrium behaviors found for a given parameterization previously found by W_0^{12}.

OSCILLATIONS

Oscillations are defined here as spatially homogeneous solutions where every neuron in a given layer is either active ($u_i > 0$) or inactive ($u_i \leq 0$) independent of the feature or position variable, i.e. $u_i(\theta, t) = u_i(t)$.

For the ring topology, the connectivity function, $w(\theta)$, was expressed as a cosine series. More generally, any integrable function $f(\vec{x})$ can be expressed in an infinite series expansion using a set of orthonormal basis functions, $B_{i_1, i_2, \ldots, i_n}(\vec{x})$, for the function space:

$$f(\vec{x}) = \sum_{i_1, i_2, \ldots, i_n} a_{i_1, i_2, \ldots, i_n} B_{i_1, i_2, \ldots, i_n}(\vec{x})$$

where $B_{i_1, i_2, \ldots, i_n}(\vec{x})$ satisfies the orthogonality relations

$$\int B_{i_1, i_2, \ldots, i_n}(\vec{x}) B_{j_1, j_2, \ldots, j_n}(\vec{x}) \mathfrak{D}(\vec{x})$$
$$= \begin{cases} 0 & \text{if } i_k \neq j_k \quad \text{for some k} \\ 1 & \text{if } i_k = j_k \quad \text{for each k} \end{cases}$$

and $\mathfrak{D}(\vec{x})$ is the integration measure on the space. Given the orthogonality of the basis functions we have $\int f(\vec{x}) \mathfrak{D}(\vec{x}) = a_{0,0,\ldots,0}$. As such the oscillations are not influenced by the topology of the feature space.

Integrating over θ, the system (3) reduces to the system of ordinary differential equations:

$$\tau_1 \frac{du_1}{dt} = -u_1(t) + W_0^{11} f[u_1(t)] - W_0^{12} f[u_2(t)] + h_1$$
$$\tau_2 \frac{du_2}{dt} = -u_2(t) + W_0^{21} f[u_1(t)] + h_2 \tag{6}$$

We summarize the conditions for monostable, bistable, and oscillatory behavior in a spatially homogeneous network given in Amari (Amari, 1977). Depending on the sign of u_1 and u_2 the system will seek to move to a corresponding equilibrium point in the (u_1, u_2) phase plane which is shifted between the quadrants by the value of h_1 and h_2. Thus depending on the value of h_1 and h_2 when $W_0^{11} \geq W_0^{12}$ the system (6) exhibits either monostable or bistable behavior. When $W_0^{11} < W_0^{12}$, the system (6) can exhibit monostable, bistable, or oscillatory behavior depending on the values h_1 and h_2.

TRAVELING WAVE SOLUTIONS

Pairs of propagating pulses in the Wilson-Cowan equations with ring topology are obtained for networks where the excitatory layer receive isotropic excitatory external input (Ben-Yishai et al., 1997). We demonstrate the existence of pulse pairs when the excitatory layer receives isotropic inhibitory external input. Single layer neural fields over the real line may demonstrate traveling front solutions (Coombes, 2005). However, in the ring topology such traveling front solutions can not occur.

When the two layer neural field (3) exhibits a pair of propagating pulse solutions, we can express the solution in terms of the stationary waveforms:

$$u_i(\theta, t) = g_i(\theta - vt), i = 1, 2$$

Where g_1 and g_2 are the wave forms in layers 1 and 2 and v is the unknown wave velocity. Introducing the new variable $y = \theta - vt$ we rewrite the system (3):

$$-v\tau_1 g_1' = -g_1(y) + \int w_{11}(y - y')f[g_1(y')]\frac{dy'}{2\pi}$$
$$- \int w_{12}(y - y')f[g_2(y')]\frac{dy'}{2\pi} + h_1 \quad (7)$$
$$-v\tau_2 g_2' = -g_2(y) + W_0^{21}f[g_1(y)] + h_2 \quad (8)$$

Where $g_i'(y) = \frac{dg_i}{dy}$. Without loss of generality we assume that the wave form in layer 1 is centered at $y = 0$ and the unknown width of the excited region is $2a$. The excited regions of the field for layer 1 and 2 are:

$$R[g_1] = (-a, a), \ R[g_2] = (y_1, y_2)$$

where $y_1 < y_2$ denote the unknown boundaries of the excited region of layer 2. Under the boundary condition $g_2(-\pi) = g_2(\pi)$ reflecting the periodic nature of the ring topology we find explicit solution to (8):

$$g_2(y) =$$
$$\begin{cases} W_0^{21}\frac{\sinh\left(\frac{a}{v\tau_2}\right)}{\sinh\left(\frac{\pi}{v\tau_2}\right)}e^{\frac{y+\pi}{v\tau_2}} + h_2 & -\pi \leq y < -a \\ W_0^{21}\frac{\sinh\left(\frac{a-\pi}{v\tau_2}\right)}{\sinh\left(\frac{\pi}{v\tau_2}\right)}e^{\frac{y}{v\tau_2}} + W_0^{21} + h_2 & -a \leq y < a \\ W_0^{21}\frac{\sinh\left(\frac{a}{v\tau_2}\right)}{\sinh\left(\frac{\pi}{v\tau_2}\right)}e^{\frac{y-\pi}{v\tau_2}} + h_2 & a \leq y < \pi \end{cases}$$

As the waveform in layer 2 trails layer 1, $0 < y_2 \leq a$. From $g_2(y_2) = 0$, y_2 is found:

$$y_2 = v\tau_2 \ln \frac{-W_0^{21} - h_2}{W_0^{21}\left(\frac{\sinh\left(\frac{a-\pi}{v\tau_2}\right)}{\sinh\left(\frac{\pi}{v\tau_2}\right)}\right)} \quad (9)$$

However, given the periodic nature of the ring topology y_1 could lie in either the region $-\pi \leq y_1 \leq -a$ or $a \leq y_1 < \pi$ depending on the layer 2 membrane properties (τ_2), strength of the drive from layer 1 to layer 2 (W_0^{21}), the width and velocity of the wave in layer 1 ($2a, v$), and the level of homogeneous input to level 2 (h_2). When $-\pi \leq y_1 \leq -a$ then $y_1 = y_a$ where:

$$y_a = v\tau_2 \ln \frac{-h_2}{W_0^{21}\left(\frac{\sinh\left(\frac{a}{v\tau_2}\right)}{\sinh\left(\frac{\pi}{v\tau_2}\right)}\right)} - \pi \quad (10)$$

Otherwise, $y_1 = y_a + 2\pi$ admissible regions.

The expressions for y_1 and y_2 imply two necessary conditions for the existence of traveling wave solutions with non-zero wave velocity for the two layer neural field model. These conditions are $h_2 < 0$ from (10) and $W_0^{21} > -h_2$ from (9). Violation of either of these necessary conditions could potentially lead to a standing wave solution in layer 1 previously described. Note that the values for y_1 and y_2 depend upon the unknown values a and v.

Given $R[g_2]$ we solve for $g_1(y)$. Rewriting (7) as:

$$-v\tau_1 g_1' = -g_1(y) + K(y) + h_1$$

where

$$K(y) = \int_{-a}^{a} w_{11}(y - y')\frac{dy'}{2\pi} - \int_{R[g_2]} w_{12}(y - y')\frac{dy'}{2\pi}$$
$$= \frac{1}{2\pi}\Big(2aW_0^{11} - W_012\Delta y + 2W_1^{11}\sin(a)\cos(y)$$
$$- 2W_1^{12}\sin\left(\frac{\Delta y}{2}\right)\cos(y - \bar{y})\Big)$$

and Δy and $\bar{y}$ are the width and center respectively of the layer 2 waveform. When $v > 0$ and $-\pi \leq y_1 \leq -a$, $\Delta y = y_2 - y_1$ and $\bar{y} = \frac{y_2 + y_1}{2}$.

With boundary condition $g_1(-\pi) = g_1(\pi)$, an explicit solution to (7) is found:

$$g_1(y) = \frac{a}{\pi}W_0^{11} - \frac{\Delta y}{2\pi}W_0^{12} + h_1$$
$$+ \frac{1}{1 + (\tau_1 v)^2}\frac{\sin(a)}{\pi}W_1^{11}\big(\cos(y) - \tau_1 v \sin(y)\big)$$
$$- \frac{1}{1 + (\tau_1 v)^2}\frac{\sin\left(\frac{\Delta y}{2}\right)}{\pi}W_1^{12}$$
$$\big(\cos(y - \bar{y}) - \tau_1 v \sin(y - \bar{y})\big)$$

From the relations $g_1(\pm a) = 0$ we numerically find the width of the active region in layer 1, $2a \approx 0.72\pi rad$, and wave velocity, $v \approx 0.19\pi rad/\tau$ for the parameter set:

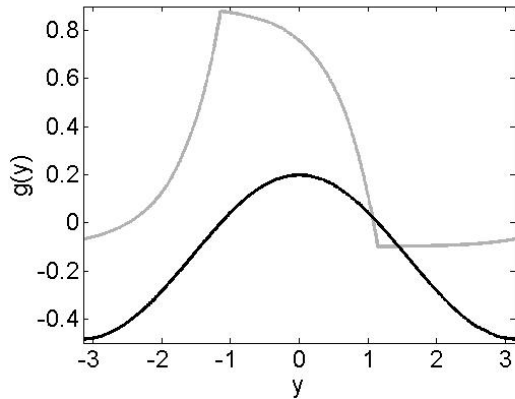$$W_0^{11} = 3, W_1^{11} = 2, W_0^{12} = 2, W_1^{12} = 1, W_0^{21} = 1,$$

Fig. 2. Waveforms for traveling wave solution with positive wave velocity. Shown are $g_1(y)$ (black line) centered at $y = 0$ and corresponding $g_2(y)$ (grey line).

$$h_1 = h_2 = -0.1, \tau_1 = \tau_2 = 1.$$

The corresponding stationary waveforms are shown in figure 2. For layer two, the boundaries for the pulse are $y_2 \approx 0.34\pi rad$ and $y_1 \approx -0.79\pi rad$ resulting in a width of the waveform in layer 2 of $\Delta y \approx 0.88\pi rad$.

The symmetry of the connectivity function allows for pulses to propagate with either a positive or negative velocity. For the analysis of propagating pulses, it was sufficient to study just the waves with positive velocity as the symmetry of the problem will yield a "mirror" result for the waves with negative velocity. That is, whenever a pair (a, v) is found that permits a traveling wave solution, the pair $(a, -v)$ will also permit a traveling wave solution.

Traveling front solutions

In both the single layer and two layer neural field models (1) under certain parameter regimes the field has two stable stationary homogeneous states. However, the boundary condition of the ring topology, $u(-\pi, t) = u(\pi, t)$, prohibits the formation of a traveling front solution. For example, a disturbance $g(\theta - vt)$ of the quiescent state with non-zero velocity v, whose width is not such that the field enters the fully active state would necessarily have a homoclinic orbit in the $\left(g(y), g'(y)\right)$ phase-plane where $y = \theta - vt$. That is, owing to the periodic nature of the boundary condition $u(\theta, t) = u\left(\theta, t + \frac{2\pi}{v}\right)$, any point where $u(\theta, t) \leq 0$ will return to this state within a time period of $\frac{2\pi}{v}$ from the disturbance. Situations where a quiescent state could be carried to a stable all active state may be highly undesirable as in a stable all active state it is very difficult to return network to a quiescent state where neurons could be responsive to new input.

DISCUSSION

Cortical neurons receive most of their input locally through synaptic interactions with other neurons that are in close physical proximity. Amari utilized this idea to develop a model for neural tissue that exhibited both spatial and dynamic pattern formation (Amari, 1977). However, VSDI and other experiments have demonstrated that cortical neurons also organize topographically on the cortical surface properties of stimulus features (Blasdel and Salama, 1986; Grinvald and Hildesheim, 2004; Hubel and Wiesel, 1977; Woolsey et al., 1942). The dual constraints of local processing and topographic representation of stimulus features have strong influence on neural computation and cortical processing. Utilizing compact topologies implied by topographic maps in cortex have shown new results in spatial pattern formation in single layer neural fields of lateral inhibition type (Haskell and Bressloff, 2003; Haskell and Paksoy, 2011). In this study a mechanism through the network interactions that generates and sustains standing and traveling waves in a two layer ring topology neural field has been explored. To what respect the ring topology is an appropriate network topology depends on the cortical area of study. However, given the dual constraints of local connectivity and network topology it is important to understand the influence that topology may have in generating the dynamic behaviors that are observed in a host of natural and pathological cortical conditions.

While the model presented takes into account both the nature of local processing and topography in cortex, the symmetry of the connectivity functions places no constraint on whether the wave velocity will be positive or negative. Traveling waves of spontaneous activity are ubiquitous in developing nervous systems, default mode fMRI studies, and evoked cortical responses. The direction of these waves may indicate an order to information flow through the nervous system that may be important in development and maintenance of normal brain function. Using the orientation tuning example, an experiment where a researcher measures the response in primary visual cortex area V1 to a rotating bar would result in a directed wave of excitation through the hypercolumn following the direction of the orientation. This is a locking of the response to the stimulus that is known to occur in populations of neurons from both experiments (Sirovich, 2012) and from theoretical considerations (Ben-Yishai et al., 1995; Knight, 1972; Sirovich, 2012). While stimulus locking can provide directionality in evoked responses, spontaneous responses may require an alternate mechanism. In area V1 it has been observed experimentally that long-range lateral connections can serve to modulate neural activity (Hirsch and Gilbert, 1991). This modulation of the local drive of the neural population could serve to provide an imbalance to the local activity that gives the wave a specific direction. The ability of the local network to support waves in any direction provides a strong constraint to the global network structure.

ACKNOWLEDGEMENTS

opment Grant award to ECH.

REFERENCES

Amari, S. (1977). Dynamics of pattern formation in lateral-inhibition type neural fields. *Biol. Cybern.*, 27:77–87.

Amit, D. and Brunel, N. (1997). Model of global spontaneous activity and local structured activity during delay periods in the cerebral cortex. *Cerebral Cortex*, 7(3):237–252.

Ben-Yishai, R., Bar-Or, R. L., and Sompolinsky, H. (1995). Theory of Orientation Tuning in Visual Cortex. *Proceedings of the National Academy of Sciences*, 92:3844.

Ben-Yishai, R., Hansel, D., and Sompolinsky, H. (1997). Traveling Waves and the Processing of Weakly Tuned Inputs in a Cortical Network Module. *Journal of Computational Neuroscience*, 4(1):57–77.

Blasdel, G. G. and Salama, G. (1986). Voltage-Sensitive Dyes Reveal a Modular Organization in Monkey Striate Cortex. *Nature*, 321:579–585.

Blomquist, P., Wyller, J., and Einevoll, G. (2005). Localized activity patterns in two-population neuronal networks. *Physica D: Nonlinear Phenomena*, 206(3):180–212.

Chen, Y., Palmer, C., and Seidemann, E. (2012). The relationship between voltage-sensitive dye imaging signals and spiking activity of neural populations in primate V1. *Journal of Neurophysiology*, 107(12):3281–3295.

Coombes, S. (2005). Waves, bumps, and patterns in neural field theories. *Biological Cybernetics*, 93(2):91–108.

Douglas, R. J., Koch, C., Mahowald, M., Martin, K. A. C., and Suarez, H. H. (1995). Recurrent Excitation in Neocortical Circuits. *Science*, 269:981–985.

Fitzgerald, J. K., Freedman, D. J., Fanini, A., Bennur, S., Gold, J. I., and Assad, J. A. (2013). Biased associative representations in parietal cortex. *Neuron*, 77(1):180–191.

Giese, M. (1998). *Dynamic neural field theory for motion perception*. Kluwer Academic Publishers.

Grinvald, A. and Hildesheim, R. (2004). VSDI: a new era in functional imaging of cortical dynamics. *Nature Reviews Neuroscience*, 5(11):874–885.

Hansel, D. and Sompolinsky, H. (1998). Modeling feature selectivity in local cortical circuits. In Koch, C. and Segev, I., editors, *Methods in neuronal modeling*, pages 499–567. MIT Press, Cambridge, MA.

Haskell, E. C. and Bressloff, P. (2003). On the formation of persistent states in neuronal network models of feature selectivity. *Journal of Integrative Neuroscience*, 2(01):103–123.

Haskell, E. C. and Paksoy, V. (2011). Localized Activity States for Neuronal Field Equations of Feature Selectivity in a Stimulus Space with Toroidal Topology. In Machado, J. A. T., Baleanu, D., and Luo, A. C., editors, *Nonlinear and Complex Dynamics: Applications in Physical, Biological, and Financial Systems*, pages 207–216. Springer, New York.

Hirsch, J. A. and Gilbert, C. D. (1991). Synaptic Physiology of Horizontal Connections in the Cat's Visual Cortex. *Journal of Neuroscience*, 11:1800–1809.

Hubel, D. and Wiesel, T. (1977). Ferrier lecture: Functional architecture of macaque monkey visual cortex. *Proceedings of the Royal Society of London. Series B, Biological Sciences*, pages 1–59.

Kass, J. H. (1997). Topographic Maps Are Fundamental to Sensory Processing. *Brain Research Bulletin*, 44:107.

Knight, B. (1972). Dynamics of encoding in a population of neurons. *Journal of General Physiology*, 59:734–766.

Nunez, P. (1995). *Neocortical dynamics and human EEG rhythms*. Oxford University Press, USA.

Pinotis, D. A., Moran, R. J., and Firston, K. J. (2012). Dynamic causal modeling with neural fields. *NeuroImage*, 59:1261–1274.

Pinto, D. and Ermentrout, G. (2001). Spatially structured activity in synaptically coupled neuronal networks: II. Lateral inhibition and standing pulses. *SIAM Journal on Applied Mathematics*, 62(1):226–243.

Purushothaman, G. and Bradley, D. (2004). Neural population code for fine perceptual decisions in area mt. *Nature Neuroscience*, 8(1):99–106.

Roerig, B. and Chen, B. (2002). Relationships of Local Inhibitory and Excitatory Circuits to Orientation Preference Maps in Ferret Visual Cortex. *Cerebral Cortex*, 12:187–198.

Salomon, F. and Haskell, E. C. (2012). Travelling wave solutions for ring topology neural fields. In Vigo-Aguiar, J., editor, *12th International Conference Computational and Mathematical Methods in Science and Engineering (CMMSE 12)*, pages 1523–1531.

Shigesada, N. and Kawasaki, K. (1997). *Biological invasions: theory and practice*. Oxford University Press, USA.

Silver, M. and Kastner, S. (2009). Topographic maps in human frontal and parietal cortex. *Trends in cognitive sciences*, 13(11):488–495.

Simoncelli, E. P. and Olshausen, B. A. (2001). Natural Image Statistics and Neural Representation. *Annual Review of Neuroscience*, 24:1193–1216.

Singh, G., Memoli, F., Ishkhanov, T., Sapiro, G., Carlsson, G., and Ringach, D. (2008). Topological analysis of population activity in visual cortex. *Journal of vision*, 8(8).

Sirovich, L. (2012). The faithful copy neuron. *Journal of Computational Neuroscience*, 32(3):377–385.

Somers, D., Nelson, S. B., and Sur, M. (1995). An Emergent Model of Orientation Selectivity in Cat Visual Cortical Simple Cells. *Journal of Neuroscience*, 15:5448–5465.

Wilimzig, C., Ragert, P., and Dinse, H. (2012). Cortical topography of intracortical inhibition influences the speed of decision making. *Proceedings of the National Academy of Sciences*, 109(8):3107–3112.

Wilson, H. and Cowan, J. (1973). A mathematical theory of the functional dynamics of cortical and thalamic nervous tissue. *Biological Cybernetics*, 13(2):55–80.

Woolsey, C., Marshall, W., and Bard, P. (1942). Representation of cutaneous tactile sensibility in the cerebral cortex of the monkey as indicated by evoked potentials. *Bull Johns Hopkins Hosp*, 70:399–441.

Wu, J., Huang, X., and Zhang, C. (2008). Propagating waves of activity in the neocortex: what they are, what they do. *The Neuroscientist*, 14(5):487–502.

Zhang, K. (1996). Representation of spatial orientation by the intrinsic dynamics of the head-direction cell ensemble: a theory. *The journal of neuroscience*, 16(6):2112–2126.

FAYSSA SALOMON holds a BS degree in Biology from Nova Southeastern University. Currently Ms. Salomon is pursuing the MS in Medical Sciences at the University of South Florida.

EVAN HASKELL is an Associate Professor of Mathematics at Nova Southeastern University. Dr. Haskell holds a Ph.D. in Mathematics from the Courant Institute of Mathematical Sciences, New York University. Previously Dr. Haskell was a visiting member of Cognitive Neuroscience sector at the International School for Advanced Study (SISSA) in Trieste, Italy, Scott Assistant Professor of Mathematics at University of Utah, and Visiting Assistant Professor of Mathematics at College of William and Mary.